Iron limitation across chlorophyll gradients in the southern Drake Passage: Phytoplankton responses to iron addition and photosynthetic indicators of iron stress

Brian M. Hopkinson
Geosciences Research Division, Scripps Institution of Oceanography, University of California, San Diego, 9500 Gilman Drive, La Jolla, California 92093-0218

B. Greg Mitchell, Rick A. Reynolds, and Haili Wang
Integrative Oceanography Division, Scripps Institution of Oceanography, University of California, San Diego, 9500 Gilman Drive, La Jolla, California 92093-0218

Karen E. Selph and Christopher I. Measures
Department of Oceanography, University of Hawaii, Honolulu, Hawaii 96822

Christopher D. Hewes and Osmund Holm-Hansen
Marine Biology Research Division, Scripps Institution of Oceanography, University of California, San Diego, 9500 Gilman Drive, La Jolla, California 92093-0202

Katherine A. Barbeau[1]
Geosciences Research Division, Scripps Institution of Oceanography, University of California, San Diego, 9500 Gilman Drive, La Jolla, California 92093-0218

Abstract

Processes influencing phytoplankton bloom development in the southern Drake Passage were studied using shipboard iron-enrichment incubations conducted across a surface chlorophyll gradient near the Antarctic Peninsula, in a region of water mass mixing. Iron incubation assays showed that Antarctic Circumpolar Current (ACC) waters were severely iron limited, while shelf waters with high ambient iron concentrations (1–2 nmol L^{-1}) were iron replete, demonstrating that mixing of the two water masses is a plausible mechanism for generation of the high phytoplankton biomass observed downstream of the Antarctic Peninsula. In downstream high-chlorophyll mixed waters, phytoplankton growth rates were also iron limited, although responses to iron addition were generally more moderate as compared to ACC waters. Synthesizing results from all experiments, significant correlations were found between the initial measurements of Photosystem II (PSII) parameters ($F_v : F_m$, σ_{PSII}, and p) and the subsequent responses of these waters to iron addition. These correlations indicate that PSII parameters can be used to assess the degree of iron stress experienced in these waters and likely in other regions where photoinhibition and nitrogen stress are not confounding factors.

Explaining the distribution of phytoplankton biomass in the Southern Ocean has long been a challenge. While the major nutrients that control production throughout much of the world's oceans are plentiful in the Southern Ocean, high phytoplankton biomass is primarily found around or downstream of islands and the continental shelf and in the Antarctic Polar Frontal Zone (Sullivan et al. 1993;

Holm–Hansen et al. 2005). Attempts to explain the causes of variability in phytoplankton biomass have focused on the availability of iron and light, the two strongest bottom-up controls on phytoplankton growth in the Southern Ocean. Well-studied seasonal blooms in the Ross Sea and the Antarctic Polar Frontal Zone are controlled by both light and iron availability (Sedwick et al. 2000; Smith et al. 2000). Light limitation prevails throughout the winter and late spring in regions with deep mixed layers (Mitchell et al. 1991). Only at the onset of stratification due to increased heating of surface layers, reduced winds, or melting of sea-ice do blooms begin to form, generally persisting for several weeks (Smith et al. 2000). Iron inputs to surface waters in regions that develop seasonal blooms occur primarily during the winter and early spring from deep mixing and melting of sea-ice, and iron levels are relatively high at the beginning of the bloom (Sedwick et al. 2000). This iron is depleted as the growing season progresses to the point that phytoplankton biomass and growth rates become iron limited, leading to bloom decline.
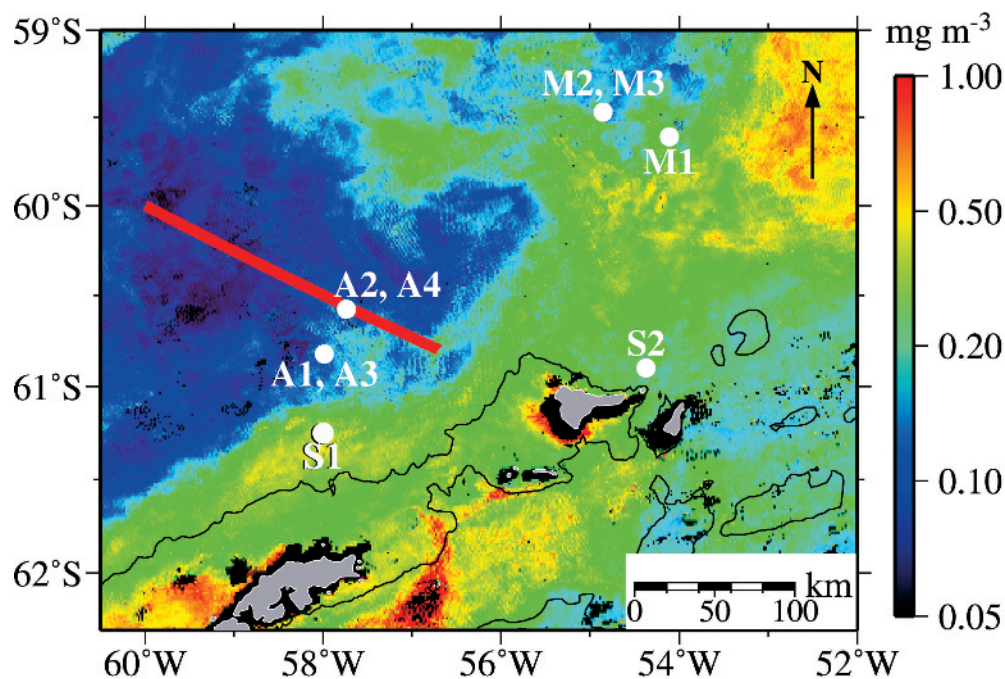
Fig. 1. Satellite chlorophyll image of the study region, with locations of incubation experiments overlain. The satellite image is a MODIS chlorophyll composite from January–March 2004, spanning the time of our study. Low-chlorophyll, iron-limited ACC waters are in the west and shelf waters are in the south around the South Shetland Islands, with a region of mixing between these two waters to the east, where chlorophyll is high. A deep gap between the southern end of the Shackleton Transverse Ridge (red line) and the continental shelf (delineated by the 500-m isobath; black line) creates a jet of ACC water, which leads to mixing between ACC and shelf waters (Zhou et al. unpubl. data).

Spring blooms are important phenomena over major areas of the Southern Ocean, but elevated phytoplankton biomass on continental shelves and near islands is more persistent throughout the summer months (Sullivan et al. 1993; Blain et al. 2001). High phytoplankton biomass around islands is especially evident in satellite images, in which low-chlorophyll regions persisting seasonally and interannually markedly contrast with high-chlorophyll waters around island masses. Because detailed time series and spatial studies of these regions of elevated chlorophyll have primarily been performed using satellite observations, there is limited direct information on the mechanisms responsible for their formation and maintenance. Proximity of these chlorophyll transitions to islands, the continental shelf, or seamounts indicates natural additions of iron as a potential cause, but changes in light availability due to stratification cannot be ruled out (Sullivan et al. 1993). Examining the influence of the Kerguelen Islands on phytoplankton distributions, Blain et al. (2001, 2007) found elevated levels of iron and chlorophyll in the island wake, but lower chlorophyll and iron outside, indicating that iron supply was responsible for the large phytoplankton blooms in the region. However, light availability was also found to be an important factor controlling phytoplankton biomass in the immediate vicinity of the islands where extremely deep mixed layers, up to 200 m in depth, were found at some stations. By reviewing the literature, Holm–Hansen et al. (2005) showed that waters over abyssal plains with low surface chlorophyll have low iron concentrations, while the higher chlorophyll waters found around topographic features, including shelves, islands, and seamounts, typically have high iron levels, measuring greater than 1 nmol L^{-1}, associations consistent with the hypothesized importance of iron in determining Southern Ocean phytoplankton distributions.

A major transition in surface chlorophyll concentration occurs in the southern Drake Passage near the Antarctic Peninsula, where an extensive region of low-chlorophyll water, which exists across the eastern South Pacific sector of the Southern Ocean, shifts to high-chlorophyll waters, which continue across the Scotia Sea to the South Sandwich Islands (Fig. 1; Sullivan et al. 1993). On a cruise to study mechanisms responsible for this chlorophyll transition in February and March 2004, the physical, chemical, and biological structure of the transition region was surveyed extensively. It was determined that low-chlorophyll Antarctic Circumpolar Current (ACC) waters are funneled through a gap in the Shackleton Transverse Ridge, a bathymetric rise extending off the Antarctic Peninsula perpendicular to ACC flow, creating a strong current (Zhou et al. unpubl. data). This jet of ACC water intrudes toward the shelf, where mixing with high-iron shelf water occurs. Additionally, in the lee of the jet, shelf water is pulled offshore and eddies are generated, leading to further mixing between the two waters. These transport and mixing processes may act as a natural iron fertilization of

ACC waters responsible for the elevated chlorophyll in the mixing region and downstream. Herein, we present results from shipboard iron-addition experiments conducted across the chlorophyll transition and in nearby shelf waters in order to assess the iron-limitation status of the phytoplankton community in each region. If iron supply induces the southern Drake Passage chlorophyll transition, we hypothesized that iron stress would be reduced across the chlorophyll front and that changes in phytoplankton community structure and photosynthetic physiology between low- and high-chlorophyll waters might be similar to responses observed in shipboard iron-addition grow-out experiments. An additional goal of this work was to conduct iron-addition experiments across gradients in iron stress in order to determine whether photosynthetic parameters, as measured by fast repetition rate fluorometry (FRRF) and photosynthesis versus irradiance (P vs. E) incubations, were robust indicators of iron limitation. Many of these photosynthetic parameters have been shown to be influenced by iron limitation, but they have primarily been studied at the extremes of iron limitation or nutrient-replete conditions in the field. The heterogeneous and evolving mesoscale structure of the southern Drake Passage presents a natural laboratory to examine the responses of photosynthetic physiology to gradients in iron stress, allowing their utility as indicators of iron stress to be assessed.

Methods

Water type assignments—In the region sampled, ACC and shelf waters were identified as the two primary water types (Zhou et al. unpubl. data). A mixing index (DW) describing the percent mixture of these two water types was calculated for each station using temperature and salinity characteristics in the upper 50 m of the water column at each station (Zhou et al. unpubl. data). Because small amounts of shelf water, which might not be resolved with the DW index, could cause large biological responses, we also used biological characteristics (chlorophyll distributions) to define water types. In particular, low surface chlorophyll with a deep chlorophyll maximum between 60 and 90 m is typical of low-productivity, iron-limited ACC waters (Holm–Hansen et al. 2005). For the purposes of this article, stations with a DW of <0.3 were considered 'ACC' when surface chlorophyll was low ($\sim$0.1 μg L^{-1}) and when a subsurface chlorophyll maximum was present, and they were considered 'Mixed' if surface chlorophyll was high (>0.8 μg L^{-1}) with no subsurface chlorophyll maximum. 'Shelf' stations had a DW of >0.85. In the figures and tables, these water types are designated 'A' (ACC), 'M' (Mixed), and 'S' (Shelf).

Experimental protocols—Water for experiments was collected using a trace metal–clean rosette system consisting of GO-Flo bottles and a CTD mounted on an epoxy-coated frame (Measures et al. unpubl. data). Immediately after the rosette was retrieved, the bottles were pressurized with ultra–high-purity nitrogen gas and water was dispensed into acid-washed incubation vessels in a clean environment.

Most incubations were conducted in 4-liter polycarbonate bottles, except for incubation M1, in which 50-liter low-density polyethylene carboys were used. For each experiment two containers were spiked with 5 nmol L^{-1} FeCl$_3$ from an acidified 75-μmol L^{-1} stock solution, and two containers were left unamended as controls. The containers were then sealed and transferred to a temperature-controlled van outfitted with banks of blue-fluorescent lights (Philips TLD 36W/18). Lights were on continuously and the van was maintained at 2–3°C to replicate ambient temperatures. Incubations from the surface mixed layer were incubated without shading in the van at an irradiance of 140–220 μmol photons m^{-2} s^{-1}, levels saturating for photosynthesis, as determined from P vs. E data.

For comparison with incubation conditions, characteristics of the in situ light environment were calculated based on mixed layer depths, measured diffuse attenuation coefficients, and the average incident surface irradiance over the cruise. Incubation light intensities were comparable to the average light intensities experienced by mixed layer phytoplankton (140–250 μmol photons m^{-2} s^{-1}) over the approximately 14-h photoperiod in our study area but lower than the 400–600 μmol photons m^{-2} s^{-1} maximal light intensity over the photoperiod. However, because incubations were conducted under continuous illumination, time-integrated daily light doses during incubation were roughly double the in situ values (Table 1). It should be noted that the use of continuous light may have modified phytoplankton community structure, since certain species are known to survive under only a limited range of photoperiod lengths (Timmermans et al. 2001). Incubations from deeper waters were shaded in an attempt to match light levels measured at the sampling depth (30–40 μmol photons m^{-2} s^{-1}), but again, because of continuous irradiance during incubation and overestimation of light levels, daily light doses were up to 10 times higher than the in situ light levels estimated assuming the deep layers sampled remained at a constant depth and no mixing occurred. Incubations were sampled every other day. Four-liter bottles were sampled under a Class 100 laminar flow hood. Fifty-liter carboys were sampled in the incubation van using a hand vacuum pump and a specially designed sampling cap to prevent contamination.

General—Chlorophyll a (Chl a) was determined fluorometrically using a methanol extraction method (Holm–Hansen and Reimann 1978). Water was filtered through a GF/F filter and was extracted in methanol overnight at 4°C. Fluorescence of the methanol extracts was measured before and after acidification to determine chlorophyll concentrations. For size-fractioned Chl a, filters (2 μm or 20 μm) were placed on a wetted filter base of either stainless steel (Millipore) or polystyrene (Nalgene) and filtrate was collected in a clean glass or polycarbonate container. Water (100–150 mL) was gravity filtered with constant swirling to keep cells suspended, and the filtration was ended when 25–50 mL of seawater remained in the funnel. The filtrate was then passed through a GF/F filter to catch all particles that were not retained on the 2-μm or 20-μm filters. Chl a was measured on the GF/F filters as described above, resulting

Table 1. Incubation source waters and station parameters. Relevant station data and initial parameters for each incubation (Inc), including water type (ACC, Antarctic Circumpolar Current), depth of sampling for incubation setup, iron (Fe) concentrations, chlorophyll a (Chl a), and mixed layer depth (MLD). Average daily light doses within the mixed layer or depth of sampling (In situ light) are presented for comparison with daily light doses while incubated (Inc. light). Initial PSII parameters ($F_v : F_m$, σ_{PSII} [$\times 10^{-20}$ m^2 photon^{-1}], τ^{-1}, and p) measured on waters collected for incubation are reported. Station numbers (Sta. No.) are included to facilitate comparisons with data from other papers published from this study.

Inc	Water type	Sta. No.	Depth (m)	MLD (m)	Fe (nmol L^{-1})	Chl a (μg L^{-1})	$F_v : F_m$	σ_{PSII}	τ^{-1} (s^{-1})	p	In situ light (mol m^{-2} d^{-1})	Inc. light (mol m^{-2} d^{-1})
A1	ACC	27	25	43	0.48*	0.15	0.22	913	182	0.36	11.3	16.0
A2	ACC	55	20	58	0.14	0.10	0.23	915	40	0.37	9.8	18.8
A3	ACC	27	85	43	0.48*	0.27	0.27	1035	162	0.33	0.3	2.5
A4	ACC	55	85	58	0.12	0.17	0.30	963	70	0.24	0.5	3.2
M1	Mixed	42	25	48	0.09	0.79	0.28	820	455	0.31	6.7	16.0
M2	Mixed	64	20	38	0.11	0.87	0.34	775	401	0.36	8.3	12.0
M3	Mixed	64	50	38	0.31	1.41	0.38	758	388	0.34	0.3	2.9
S1	Shelf	3	20	31	1.74	0.90	0.50	815	164	0.42	9.1	18.8
S2	Shelf	57	20	50	1.59	0.44	0.42	558	412	0.40	8.0	18.8

* May not be representative of iron concentrations in incubation water. See Methods.

in concentrations of Chl a in the <2-μm and <20-μm size fraction. Chl a in the <2-μm, 2–20-μm, and >20-μm size fractions was determined by mass balance with total Chl a.

Particulate organic carbon (POC) and particulate organic nitrogen were determined using a CHN elemental analyzer. Samples were collected by filtering 1–2 liters of water though a precombusted GF/F filter; samples were then stored in liquid nitrogen until analysis. Nutrients (NO_3, NO_2, NH_3, PO_4, and Si) were analyzed on an autoanalyzer using standard colorimetric methods. Iron measurements were made using a flow injection analysis system, as described in Measures et al. (1995), and detailed analyses of trace-metal distributions in the region will be discussed in Measures et al. (unpubl. data). Reported iron concentrations (Table 1) are taken from rosette cast profiles immediately prior to the casts used for collecting incubation water at the same station. For most stations these values should be representative of iron concentrations in incubation source waters. However, water for incubations A1 and A3 was collected in a region with sharp spatial gradients in water properties. The relatively high iron concentrations reported for these incubations (Table 1) are not likely to be representative of actual incubation water based on the strong responses observed to iron addition and the initial community measurements of photosynthetic parameters measured on actual incubation waters (*see Results and discussion*).

High-performance liquid chromatography (HPLC) pigments—Samples for HPLC analysis of phytoplankton pigments were collected on GF/F filters and stored in liquid nitrogen until analysis. HPLC analysis of pigments using a C8 column separation method was conducted at CHORS/SDSU (Van Heukelem and Thomas 2001). The CHEMTAX program was used to estimate the contribution of different phytoplankton taxa to total Chl a (Mackey et al. 1996). Taxa known to be present in Antarctic waters (diatoms, haptophytes, dinoflagellates, cryptophytes, prasinophytes, and chlorophytes) were included in the analysis using initial pigment ratios for each taxa determined for Antarctic waters by Wright et al. (1996).

FRRF—A Chelsea Fastracka FRR Fluorometer was used to measure the kinetics of fluorescence induction and decay on incubation algal assemblages, and the response was fitted to estimate Photosystem II (PSII) parameters. All samples were dark acclimated for at least 1 h prior to analysis and were then circulated through the measurement path of the instrument using a peristaltic pump. The flash protocol consisted of a single turnover saturation phase in which 100 flashlets of 1.46-μs duration were delivered at intervals of 2.8 μs, followed by a relaxation phase consisting of 20 flashlets of the same duration at 51.6-μs spacing. Sets of 15 flash sequences were internally averaged as a single acquisition, and 100 such acquisitions were obtained for each sample and were subsequently averaged to obtain high signal to noise fluorescence response curves (Fig. 2).

A set of detailed characterization experiments to determine fluorescence baseline and instrument biases were conducted onboard using the identical flash protocol employed for samples, following the procedure described in Laney (2003). Blanks at each gain setting were measured using both deionized water (Millipore) and 0.22-μm–filtered seawater. While some investigators have reported differences between these blanks (Cullen and Davis 2003), no significant differences were observed in this study. Because of the relatively high chlorophyll concentrations in our incubation samples, the magnitude of the blank was small compared to the measured signal, generally <0.2% and always <4% of the sample maximal fluorescence. Time-dependent responses in fluorescence detection were also assessed and corrected for using measurements of an inert fluorochrome, Rhodamine B.

The averaged fluorescence responses were fitted to the Kolber et al. (1998) physiological model of variable fluorescence using v5 software (Laney 2003). The output included fitted values for the minimal (F_o) and maximal (F_m) fluorescence yields; the effective absorption cross-section for PSII (σ_{PSII}); the connectivity between PSII reaction centers (p), which was allowed to range between 0 and 1; and the turnover time (τ) of PSII, which was
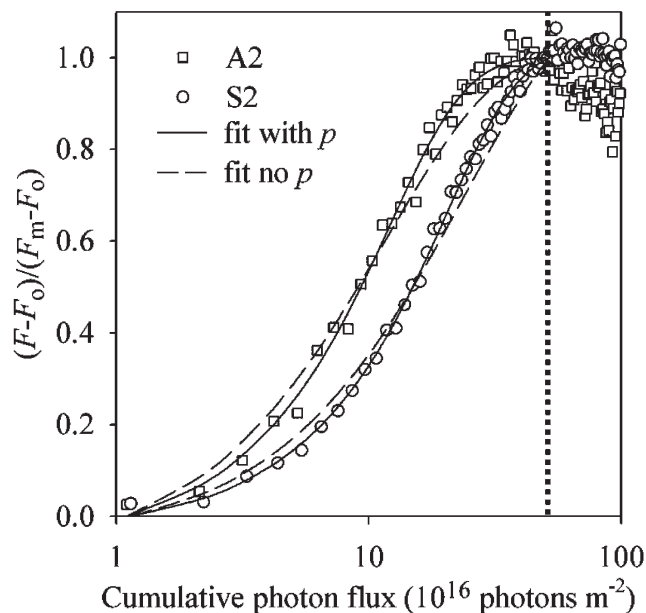
Fig. 2. Representative fluorescence response data from initiations of incubations A2 and S2 plotted to highlight the differences in σ_{PSII} between iron-limited (A2) and iron-replete (S2) waters as well as the effect of the p parameter on fits to the Kolber et al. (1998) model. Runs of the v5 fitting software with and without the p parameter demonstrate that the data are better fitted with the p parameter as a result of lowered fluorescence early in the flash sequence and later because of a more rapid rise in fluorescence than would be expected without photosystem connectivity. Note that reductions in fluorescence toward the end of the flash sequence were observed when σ_{PSII} was large (e.g., A2), in which case only data from the first 50 flashlets (before the dotted line) were fit.

modeled as a single exponential decay. $F_v : F_m$, a measure of the efficiency of photochemistry in PSII, is calculated as $(F_m - F_o)/F_m$. Light intensities in the measurement chamber were calibrated by the manufacturer (Chelsea) in order to calculate absolute values of σ_{PSII}. The model fit for each sample was examined visually to ensure a reasonable coherence with the data, and comparisons between model fits with and without the p parameter confirmed that p was used to compensate for deviations from a Poisson distribution during the rise to F_m (Fig. 2). Additionally, as shown in Fig. 2, samples with larger σ_{PSII} often exhibited reductions in fluorescence toward the end of the saturation flash sequence, in which case only the first 50 saturation flashlets were used as input to the model.

Photosynthesis versus irradiance—[14]C photosynthesis-irradiance experiments (P vs. E) were performed in a modified photosynthetron at in situ or incubation van temperature, as appropriate, for 1–2 h (Lewis and Smith 1983). Samples were acidified and degassed overnight to remove inorganic ^{14}C, and fixed ^{14}C was measured by liquid scintillation counting. Experimental data were normalized to Chl a and fit to the Platt et al. (1980) model to calculate α^{Chl}, P_{max}^{Chl}, and the light saturation parameter ($E_k = P_{max}^{Chl}/\alpha^{Chl}$). The photoinhibition parameter was set to zero if no significant photoinhibition was found.

Flow cytometry—Samples (50 mL) were collected from incubations and stored on ice in the dark until analyzed by flow cytometry within 1–6 h of collection. The flow cytometer used was a Beckman–Coulter XL, equipped with a 15-mW, 488-nm argon ion laser and mated to an Orion syringe pump for quantitative sample delivery. In order to estimate phytoplankton biomass, the normalized forward light scatter signature was calibrated for cell size, allowing estimation of a diameter for each particle. Diameters were converted to spherical volumes, with the volumes used to estimate carbon biomass per cell, using the Menden–Deuer and Lessard (2000) general equation for protist plankton, thus: log pg C cell^{-1} = 0.860 × log(volume) − 0.583. Because cells >20 μm in diameter had the maximum forward scatter signal recorded by the flow cytometer, cells in this size range were set equal to the biovolume of 20-μm cells, and the calculated biomass from these cells is considered a conservative estimate.

Iron-limitation indices (ILIs)—To quantify the degree of iron stress at each incubation station, the ratio of Chl a, POC, or Chl a–derived growth rate (μ) in iron-addition treatments was normalized to the respective value in the control treatments to produce an ILI: ILI_{Chl}, ILI_{POC}, ILI_μ, respectively (Table 2; similar to Firme et al. 2003). Generally, POC samples were only taken on the final day of each experiment (days 7–14), and so data to compute both ILI_{Chl} and ILI_{POC} were taken from the final time point so that the indices could be compared directly. Growth rates to calculate ILI_μ were determined by linear regression through natural log-transformed Chl a data from the time period of exponential growth.

Results and discussion

A total of nine incubations were conducted during the cruise: four in ACC waters, three in 'Mixed' waters, and two on the continental shelf (Fig. 1). Upper mixed layer water was used in the majority of the experiments, but two ACC water incubations were from the subsurface chlorophyll maximum, and one 'Mixed' water incubation was taken from the lower euphotic zone (Table 1). Incubation responses varied among the water types, but in a given water type, results from different incubations were similar (Tables 2–4). A synthesis of all experimental results is discussed in the following text, and Figs. 3–5 will illustrate one incubation typical of each water type.

ACC water incubations—Phytoplankton assemblages from the extremely low-iron (as low as 0.1 nmol L^{-1}; Measures et al. unpubl. data) and low-phytoplankton biomass (0.1–0.25 μg L^{-1} Chl a) ACC waters responded strongly to iron additions, consistent with previous observations in this region (Helbling et al. 1991). After a 2-d lag period Chl a began to increase at a rapid rate in the iron treatments, but it increased at a much slower rate in the controls, although there was a consistent increase throughout the control experiments (Fig. 3A). POC concentrations were higher in iron treatments, although the magnitude of the response was proportionally less than that of Chl a, as

Table 2. Basic incubation responses. Growth rates determined from Chl *a* increases (μ_{Chl}) and nitrate drawdown (μ_{NO_3}) for control (C) and iron-addition (Fe) treatments, POC levels, iron-limitation indices (ILIs), and nutrient drawdown ratios ($\mu mol\ L^{-1} : \mu mol\ L^{-1}$) from each incubation. The length of each incubation (t_f) is also reported. 'No data' (nd) indicates sufficient nutrient data was not available to compute NO_3-derived growth rates or nutrient drawdown ratios from these incubations (A2, A4).

Inc	t_f (d)	μ_{Chl} (d^{-1})		μ_{NO_3} (d^{-1})		POC ($\mu mol\ L^{-1}$)			ILI_{Chl}	ILI_{POC}	ILI_μ	$Si:NO_3^-$ drawdown		$NO_3^- : PO_4^{3-}$ drawdown	
		C	Fe	C	Fe	t_0	C	Fe				C	Fe	C	Fe
A1	12	0.14	0.39	0.12	0.29	3.8	19	54	7.4	2.9	2.9	2.06	0.97	10.3	13.2
A2	14	0.15	0.32	nd	nd	2.8	17	43	6.0	2.6	2.1	nd	nd	nd	nd
A3	11	0.18	0.47	0.25	0.37	4.5	20	66	10.0	3.3	2.6	2.73	1.17	9.7	14.4
A4	14	0.14	0.34	nd	nd	3.2	16	104	11.7	6.5	2.4	nd	nd	nd	nd
M1	13	0.11	0.24	0.18	0.25	9.6	39	76	3.4	2.0	2.3	1.82	0.98	14.9	13.5
M2	11	0.08	0.23	0.14	0.29	5.7	34	90	4.3	2.6	2.7	1.73	0.94	10.7	12.7
M3	7	0.17	0.34	0.20	0.31	11	41	62	3.0	1.5	1.9	1.94	1.12	9.9	12.2
S1	12	0.19	0.21	0.30	0.31	11	52	52	1.2	1.0	1.1	1.06	0.84	14.6	15.2
S2	14	0.37	0.42	0.40	0.40	4.0	117	139	1.3	1.2	1.1	0.82	0.77	10.6	11.0

shown by comparisons of ILI_{Chl} and ILI_{POC} for each experiment (Table 2). Cellular Chl *a* levels are reduced under iron limitation, most likely accounting for the difference in the magnitude of Chl *a* and POC responses. Higher POC : Chl *a* ratios in controls (184–324 g : g), as compared with iron treatments (66–132 g : g), provide support for this interpretation, although it should be noted that detritus and heterotrophs are included in POC measurements.

Chl *a*- and NO_3^--derived growth rates (μ_{Chl} and μ_{NO_3}), determined by linear regression of log-transformed data, were similar and were clearly affected by iron addition (Table 2). μ_{Chl} values were higher, on average, than μ_{NO_3} values for iron treatments, but they were lower than μ_{NO_3} for control treatments, which can be attributed to changes in cellular Chl *a* content, depending on iron availability. $Si : NO_3^-$ drawdown ratios were high in controls, a frequently observed consequence of excess silicification in iron-limited diatoms (Hutchins et al. 1998). In contrast, iron treatments had $Si : NO_3^-$ drawdown ratios near 1, the typical ratio observed in nutrient-replete diatoms (Table 2). Pigment data indicate that diatoms dominated

both control and iron treatments such that bulk nutrient drawdown ratios primarily reflect the activity of diatoms (Table 3; Fig. 3H). Deviations from Redfield nitrogen : phosphorus (N : P) ratios have been observed in some Southern Ocean blooms and incubation experiments, and we also found lower $NO_3^- : PO_4^{3-}$ drawdown ratios in the control treatments, possibly as a result of increased P content of iron-stressed phytoplankton (Table 2; De Baar et al. 1997; Price 2005). While incubation assemblages do not precisely replicate water column communities, the nutrient-depletion processes observed here likely operate in situ, as manifested by the large-scale depletion of Si relative to NO_3 in the Southern Ocean (Sarmiento et al. 2004).

The photosynthetic physiology of the phytoplankton assemblage was assessed at each incubation sampling with FRRF, and less frequently with P vs. E measurements. $F_v : F_m$, the maximum quantum yield for PSII photochemistry, increased after iron addition to maximum values of 0.36–0.44, but it declined toward the end of the experiments, presumably as a result of resumed iron stress after depletion of added iron by uptake, precipitation of iron oxides, or wall adsorption (Fig. 3C). The initial increase in

Table 3. Community structure response in incubations. Data are averages and standard deviations from all incubations in a given water type. Size-fractioned data are percent of Chl *a* in each size class, and taxonomic divisions are percent contribution to total Chl *a* determined with CHEMTAX. Haptophytes (Hapt.) and diatoms comprised the majority of the community in all incubations.*

Water type	Sample	<2 μm	2–20 μm	>20 μm	Hapt.	Diatoms
ACC	t_0	15 ± 7	31 ± 9	54 ± 3	48 ± 25	48 ± 26
	C	4 ± 1	20 ± 5	76 ± 5	9 ± 6	89 ± 8
	Fe	1 ± 1	21 ± 3	79 ± 3	4 ± 1	91 ± 5
Mixed	t_0	4 ± 1	20 ± 4	76 ± 5	27 ± 6	72 ± 6
	C	2 ± 1	22 ± 10	76 ± 11	22 ± 10	76 ± 11
	Fe	1 ± 1	20 ± 8	79 ± 8	9 ± 4	86 ± 6
Shelf	t_0	14 ± 6	68 ± 22	17 ± 16	24 ± 8	64 ± 20
	C	1 ± 1	15 ± 4	84 ± 4	5 ± 7	81 ± 7
	Fe	0 ± 0	15 ± 3	85 ± 3	8 ± 11	77 ± 10

* ACC, Antarctic Circumpolar Current; C, control; Fe, iron addition.

Table 4. P vs. E data. The initial slope of P vs. E curves, α^{Chl} (mg C mg Chl a^{-1} h^{-1} [μmol photons m^{-2} h^{-1}]$^{-1}$), and the maximum rate of photosynthesis, P_{max}^{Chl} (mg C mg Chl a^{-1} h^{-1}) from all incubations at the initial time point (t_0) and the final time point for the control (C) and iron treatment (Fe). Only one replicate from each treatment was sampled. nd, no data.

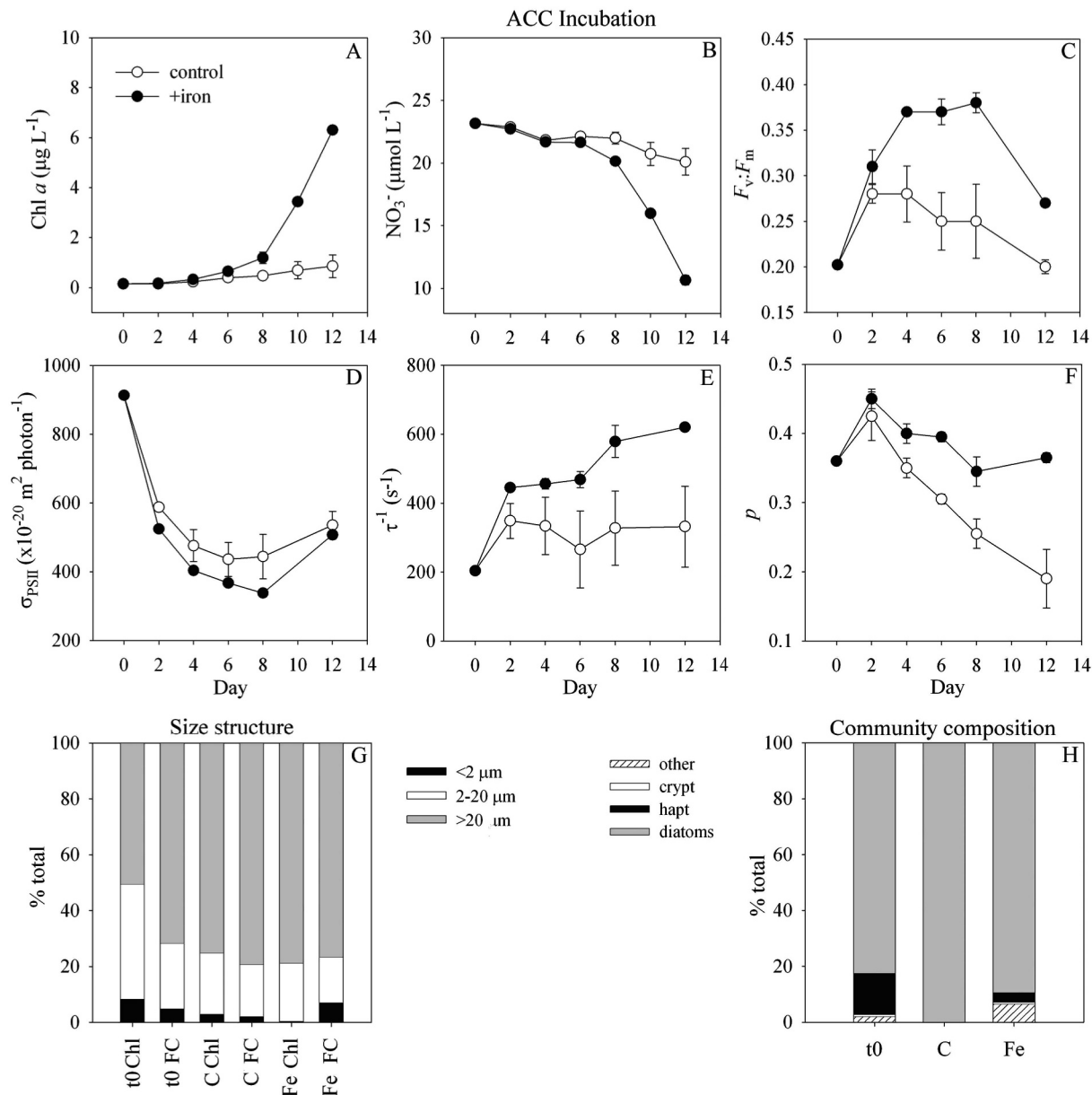| Incubation	α^{Chl}			P_{max}^{Chl}		
	t_0	C	Fe	t_0	C	Fe
A1	0.012	0.006	0.007	0.80	0.50	0.70
A2	0.031	0.010	0.013	0.35	1.00	0.90
A3	0.018	0.006	0.011	0.84	0.33	0.54
A4	0.004	0.007	0.017	0.23	0.78	1.13
M1	0.009	0.005	0.006	1.01	1.08	0.69
M2	0.014	0.003	0.007	0.99	0.37	0.74
M3	0.025	0.007	0.012	0.86	0.20	0.72
S1	nd	0.013	0.011	nd	0.91	0.80
S2	0.013	0.009	0.010	0.54	0.93	0.80

Fig. 3. (A–H) Results of a typical incubation (A1) from ACC surface waters. Error bars (A–F) are standard deviations between duplicate bottles. Size structure (G) was determined using both size-fractioned Chl *a* (Chl) and flow cytometry (FC) at the initiation of the experiment (t0) and the final time point in control (C) and iron treatments (Fe). Phytoplankton community composition (H) was determined from CHEMTAX analysis of pigments taken from the initiation of the experiment and the final time point. The 'other' category includes dinoflagellates, prasinophytes, and chlorophytes, which rarely contributed substantially to total biomass individually. Size (G) and community structure (H) data are the averages from duplicate bottles.

control $F_v : F_m$ indicates that a slight iron contamination may have occurred, potentially accounting for the small amount of growth observed in the control bottles. The PSII target size, σ_{PSII}, dropped precipitously in both treatments during the first few days of incubation, after which iron treatments had slightly but consistently smaller σ_{PSII} sizes (Fig. 3D). Because Chl *a* levels did not change in the first few days of the experiment, and because pigment data from several incubations showed only minor changes in community structure after slight increases in Chl *a* (data not shown), the decline in σ_{PSII} presumably occurred prior to major changes in phytoplankton community structure. This indicates a strong physiological acclimation of σ_{PSII} as a result of interactions between changing light and iron availability. The rapid initial drop in σ_{PSII} is probably caused by higher light doses under incubation conditions than were experienced in situ, and smaller σ_{PSII} sizes are commonly found under iron-replete conditions (Greene et al. 1992; Suzuki et al. 2002). The electron transfer rate through PSII, τ^{-1}, increased in both treatments, but to
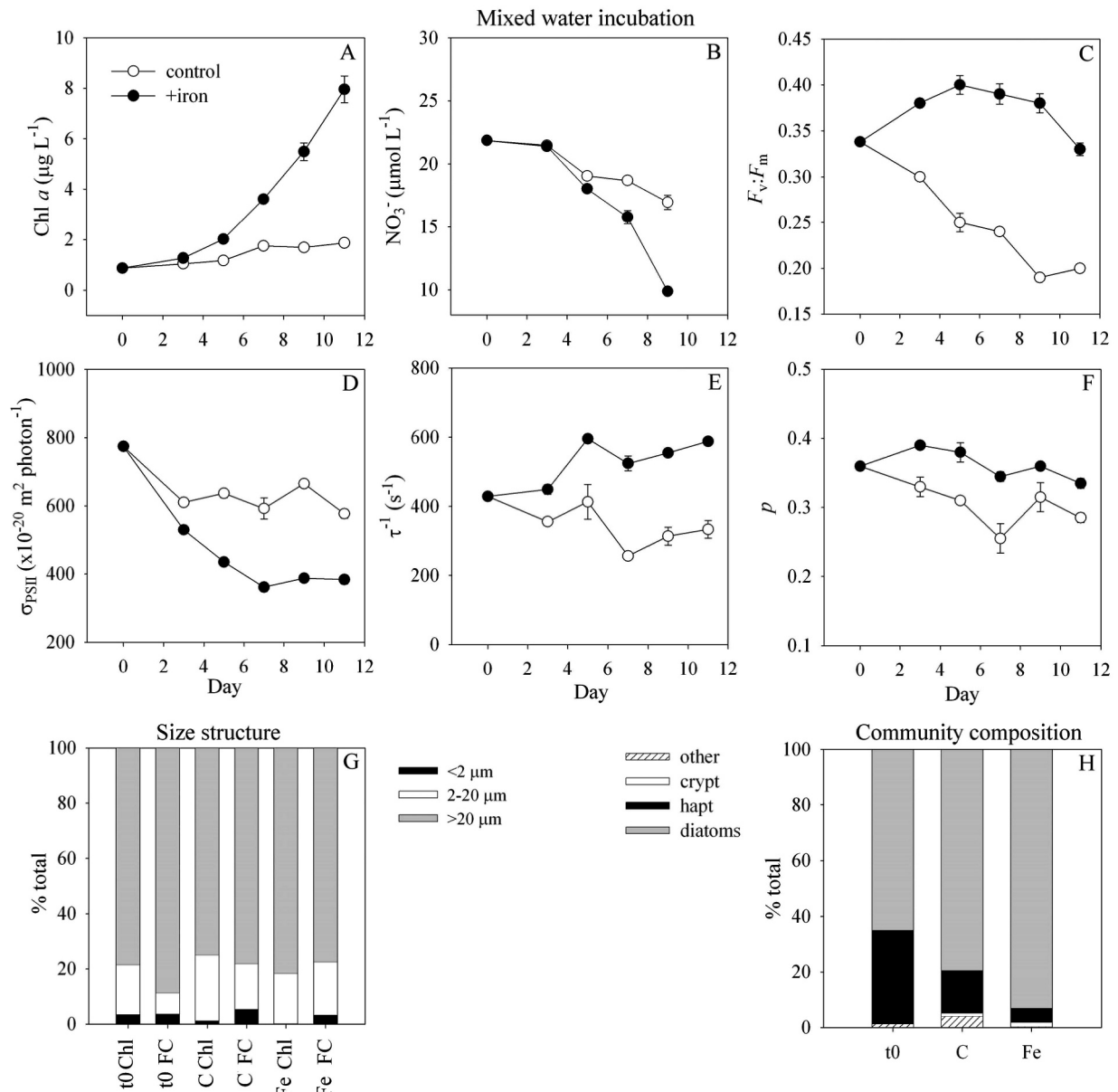
Fig. 4. (A–H) Incubation (M2) results from a 'Mixed' water experiment. Error bars (A–F) are standard deviations between duplicate bottles. Size (G) and community structure (H) show data from initial and final time points, as described in detail in the caption to Fig. 3.

a greater extent in iron treatments than in controls (Fig. 3E). p, the degree of connection between photosynthetic units, was initially moderately high but dropped off over the course of the incubation in control treatments, while remaining constant in iron treatments (Fig. 3F), consistent with culture studies showing that iron limitation reduces p (Greene et al. 1992; Vassiliev et al. 1995).

The behavior of P vs. E parameters varied among ACC experiments. The initial slope of the P vs. E curves, α^{Chl}, generally declined during incubations, perhaps as a result of elevated light doses during incubation, but this value was often higher at the end of experiments in iron treatments (Table 4). There were no clear trends in the behavior of P_{max}^{Chl}, the maximum rate of photosynthesis, but in three out

of four ACC water experiments P_{max}^{Chl} was higher in iron treatments by the end of the experiment. The normalization of α^{Chl} and P_{max}^{Chl} to Chl a, which changes on a cellular basis depending on iron stress or light level, may obscure cellular photosynthetic responses to iron, but alternative normalization variables, including POC and flow cytometry–derived carbon biomass, are also problematic because of detrital material included in POC and maximal size estimates available from flow cytometry (*see Methods*). While results varied significantly between experiments, the higher P_{max}^{Chl} and α^{Chl} values generally observed in iron treatments are consistent with results from laboratory culture experiments testing the effects of iron limitation on photosynthetic physiology (Greene et al. 1991).
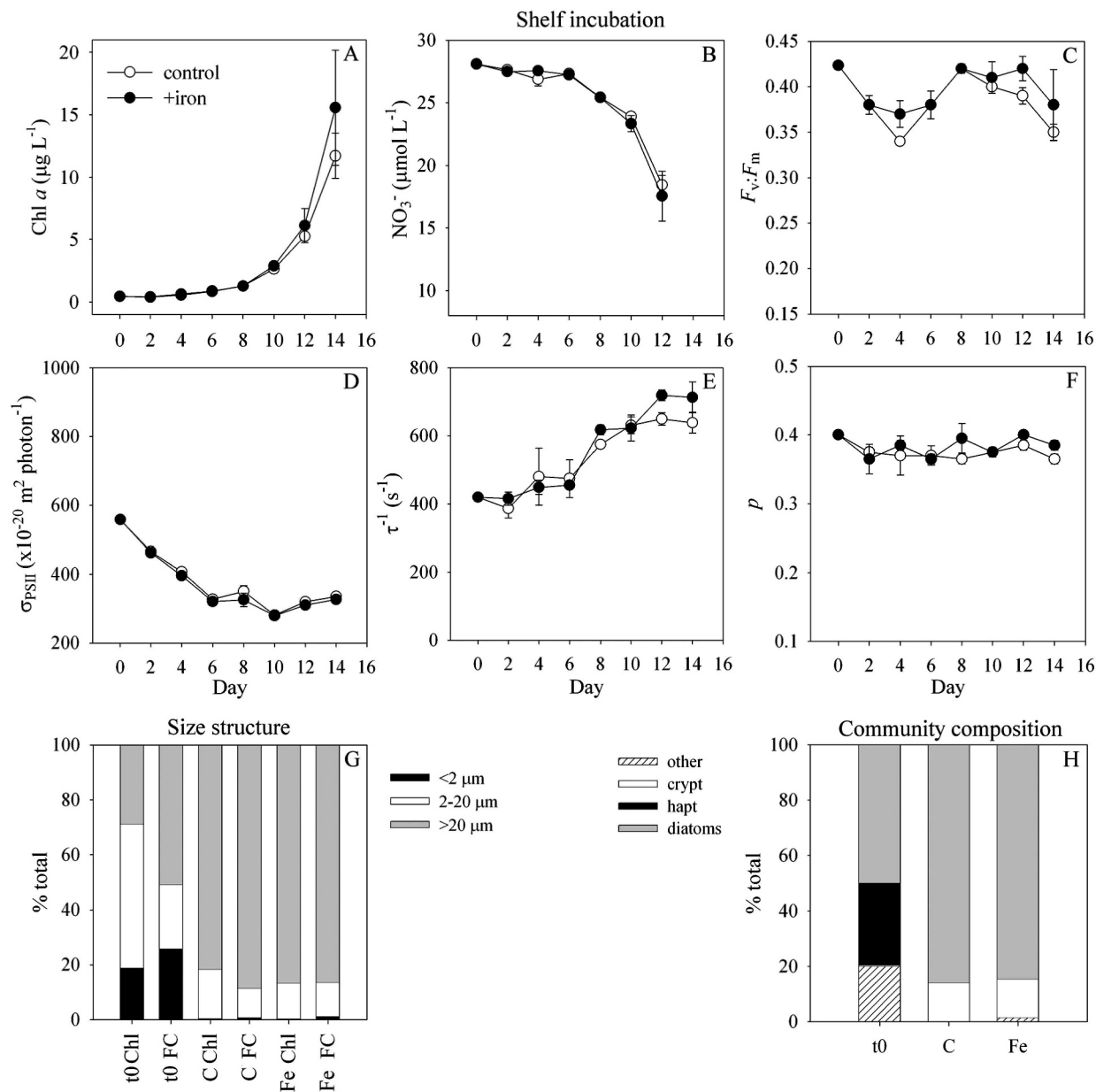
Fig. 5.   Incubation (S2) results from a shelf experiment. Error bars (A–F) are standard deviations between duplicate bottles. Size (G) and community structure (H) show data from initial and final time points, as described in detail in the caption to Fig. 3.

Phytoplankton community and size structure were not significantly different between control and iron treatments, but shifts to larger-sized phytoplankton and diatom dominance were seen, compared to the initial community (Table 3; Fig. 3G,H). As determined by CHEMTAX analysis of HPLC pigment data, diatoms were initially abundant, though variations between experiments were large (Table 3). These observations are consistent with historical data showing that diatoms tend to dominate phytoplankton communities in these waters, though in some years flagellate-dominated communities have been observed (Villafane et al. 1995). As is typically observed in iron-addition incubations, diatoms came to dominate iron treatments, contributing >80% to Chl *a* in all cases.

However, because diatoms were already abundant in initial communities, changes in community structure were less dramatic than is often observed. Diatoms also dominated control treatments, and the lack of difference between iron and control treatments may be due to various factors, including slight iron contamination of controls or effects of bottle confinement on community dynamics. In particular, grazing pressure was likely reduced on larger phytoplankton, such as diatoms, because of underrepresentation of mesozooplankton. Size-fractioned Chl *a* and flow cytometry both illustrate the abundance of large cells in initial communities and incubation treatments (Fig. 3G; Table 3). At more than 50% of total Chl *a*, the proportion of the initial phytoplankton community in the >20-μm size

fraction is somewhat greater than has typically been found in low-chlorophyll Antarctic waters (e.g., Villafane et al. 1995), although methodological differences make comparisons between size-fractioned measurements difficult.

Mixed waters—Although initial phytoplankton biomass was elevated in the 'Mixed' waters (0.8–1.4 μg Chl a L^{-1}) compared to ACC waters, iron concentrations were similarly low in the 0.1–0.3 nmol L^{-1} range (Table 1; Measures et al. unpubl. data). The 'Mixed' water stations in which incubations were started comprised predominantly ACC water (DW < 0.3), well off the shelf break, with apparently only small amounts of shelf water mixed in (Fig. 1; Zhou et al. unpubl. data). Clear responses were observed upon addition of iron to 'Mixed' waters, responses that were qualitatively similar to those in ACC waters but that were lesser in magnitude, as shown by the ILI values computed for each incubation (Table 2). Chl a and POC increased in both iron and control treatments, but did so at a more rapid rate in bottles with added iron, indicating that net growth rates in these waters could be iron limited (Fig. 4A; Table 2). Si : NO$_3^-$ drawdown ratios were nearly 2 in control treatments in all 'Mixed' water incubations, a finding that is indicative of iron-limited diatom growth, while drawdown ratios in iron treatments returned to 1 (Table 2). Pigment data showed that diatoms dominated growth in both control and iron treatments, and so drawdown ratios should largely reflect diatom physiology (Table 3). The response of NO$_3^-$: PO$_4^{3-}$ drawdown ratios to iron addition was not consistent among 'Mixed' water experiments. In two 'Mixed' water experiments, NO$_3^-$: PO$_4^{3-}$ drawdown ratios were lower in control treatments, as was found in ACC water incubations as well. However, one 'Mixed' water experiment did not show a difference in NO$_3^-$: PO$_4^{3-}$ drawdown ratios between treatments.

Photosynthetic parameters in iron and control treatments diverged, becoming characteristic of iron limitation in controls (Fig. 4). $F_v : F_m$ was initially 0.28–0.38, intermediate between the low values found in ACC waters and the higher values found on the shelf (Table 1). In iron treatments $F_v : F_m$ stayed high throughout the experiment, increasing slightly after iron addition and falling moderately in the final days of the incubation (Fig. 4C). $F_v : F_m$ declined in controls over the course of the experiment. Photoinhibition at elevated incubation light levels may have contributed to the decline, but the duration of the decline and the strong separation between iron-addition and control treatments indicates that increasing iron stress in controls was also important. The results indicate that the moderately low $F_v : F_m$ in 'Mixed' waters is due to more mild iron stress relative to ACC waters. p roughly followed the behavior of $F_v : F_m$ (Fig. 4F), and τ^{-1} increased in iron treatments, while decreasing in controls, again indicating relief of iron limitation after supplementation with iron and increased iron stress in controls as macronutrients are depleted (Fig. 4E; Greene et al. 1991, 1992). As in the ACC water experiments, a drop in σ_{PSII} occurred in the first few days of the incubation. However, σ_{PSII} in iron treatments continued to fall, leveling off at a much lower value than in

the controls, creating greater separation between treatments than was seen in the ACC experiments (Fig. 4D). This may be due to differences in the response of each community to the interacting influences of iron and light, perhaps affected by the initial iron-limitation status or community composition of the phytoplankton. P$_{max}^{Chl}$ and α^{Chl} were higher in iron treatments for incubations M2 and M3 as a result of declines in control bottles over the course of the incubation, which may be the result of the combined effects of increasing iron stress and elevated incubation light doses (Table 3). However, in M1, P$_{max}^{Chl}$ and α^{Chl} did not change a great deal during incubation, except for a small decline in P$_{max}^{Chl}$ in the iron treatment.

Large diatoms dominated 'Mixed' waters initially and continued to grow in both control and iron treatments. Pigment, particle count, and size-fractioned Chl a data indicated there were only small shifts in community composition and size structure between the initial and final communities, and no differences between control and iron treatments (Fig. 4G,H; Table 2).

Shelf waters—On the continental shelf, ambient iron concentrations were high (1–2 nmol L^{-1}) making iron limitation unlikely (Table 1; Measures et al. unpubl. data). In incubations initiated from shelf waters, no differences between control and iron treatments were observed, even after strong growth and macronutrient drawdown (Fig. 5). Chl a and POC increased rapidly in all treatments, indicating that iron was not limiting in shelf waters and was present in sufficient quantities to allow macronutrients to be depleted significantly (Fig. 5A,B). Initial photosynthetic parameters were characteristic of healthy, growing cells and remained so throughout the incubations. Presumably as a result of the incubation light regime, τ^{-1} increased and σ_{PSII} decreased during the experiment (Fig. 5D,E). $F_v : F_m$ and p remained at high values throughout the experiment, and there were no differences between iron and control treatments for any of the PSII parameters (Fig. 5C–F). The size structure of the initial shelf phytoplankton communities was distinctly smaller than ACC and 'Mixed' water, despite relatively high biomass, with Chl a mostly in the nanoplankton (2–20-μm) size class (Fig. 5G; Table 3). However, during incubation, microplankton (>20 μm) growth was most rapid, reaching >80% of size-fractioned Chl a by the end of the experiments (Fig. 5G; Table 2). Taxonomic composition of phytoplankton at the start of experiments was variable, with diatoms dominating incubation S1 and with haptophytes and diatoms in roughly equal proportions in S2, but diatoms were most successful under incubation conditions in both experiments (Fig. 5H; Table 3).

Despite high iron and macronutrient concentrations, phytoplankton biomass was relatively low on the shelf for the month-long duration of our cruise, although at 0.4–1.0 μg Chl a L^{-1} it was still higher than ACC waters and similar to 'Mixed' waters. Because shelf waters were weakly stratified and because deep mixed layers are often observed, light availability is a potential constraint on phytoplankton growth (Mitchell et al. 1991). The smaller size of phytoplankton found on the shelf is also consistent with

light stress, as smaller phytoplankton with greater surface area to volume ratios are more successful at harvesting light under low-light conditions. However, grazing pressure on larger phytoplankton from abundant krill may also alter the phytoplankton community size structure and potentially limit increases in phytoplankton standing stocks (Haberman et al. 2003). Although we are not able to thoroughly assess limitations on shelf phytoplankton biomass in this analysis, identifying constraints on shelf biomass is important, not only for the shelf ecosystem, but also for understanding conditions allowing bloom development after the mixing of ACC and shelf waters. The lack of significant phytoplankton growth and iron utilization may maintain high iron concentrations on the shelf, allowing shelf waters to serve as an iron source to the ACC (Measures et al. unpubl. data).

Natural iron fertilization in the southern Drake Passage— These incubation experiments were conducted as part of an interdisciplinary project designed to test the hypothesis that natural iron fertilization of ACC waters is occurring in the southern Drake Passage. The experimental results from our 2004 cruise indicate that phytoplankton growth rate and ultimate biomass, in the absence of other limiting factors, were limited by iron in both the ACC and 'Mixed' waters in the southern Drake Passage, while shelf waters were iron replete, potentially serving as a source of iron to ACC waters. Because of increased light doses, the continuous photoperiod experienced by phytoplankton in incubations (Table 1), and inevitable undersampling and disturbance of the zooplankton community, these incubations on their own cannot be used to assess the influence of grazing and light limitation, nor do they replicate in situ community development. However, their utility as assays of iron stress has been validated by mesoscale enrichment experiments (e.g., Coale et al. 2004), and we employ them as a component of a multidisciplinary study to understand the regional processes controlling phytoplankton distributions. Our incubation results complement physical data from the study area, which show that ACC waters are funneled through a gap in the Shackleton Transverse Ridge, a bathymetric rise nearly perpendicular to ACC flow that begins at the tip of the Antarctic Peninsula, creating a strong current that resulted in mixing between ACC and shelf waters in the region to the east of the gap (Measures et al. unpubl. data; Zhou et al. unpubl. data; Fig. 1). Incubation experiments demonstrate that mixing of a small amount of high-iron shelf water with severely iron-depleted ACC waters is a plausible mechanism for creation of the higher phytoplankton biomass found downstream in the ACC.

Many of the differences in phytoplankton physiology and community structure between ACC and 'Mixed' waters were replicated by experimental addition of iron to ACC waters, helping to support the hypothesis that 'Mixed' water blooms were the result of natural iron additions to ACC waters. The principal distinctive characteristic of 'Mixed' waters, increased phytoplankton biomass, was clearly a response to iron in incubation experiments. Higher Chl a and POC concentrations were found in iron

treatments, compared with controls, in all ACC water experiments (Fig. 3; Table 2). PSII parameters also showed distinct responses to experimental additions of iron, and similar variations between ACC and 'Mixed' waters were evident (Table 1). Near-surface waters collected for incubation experiments initially had higher $F_v : F_m$ and faster electron transfer rates (τ^{-1}) in 'Mixed' waters compared to ACC waters, trends similar to those found in response to iron addition to ACC waters (Table 1; Fig. 3). σ_{PSII} sizes were smaller in 'Mixed' waters, and slightly lower σ_{PSII} values were seen in iron treatments compared to controls in ACC incubations (Table 1; Fig. 3D). Although the PSII parameter trends between control and iron treatments are clearly similar to the trends between ACC and 'Mixed' waters, the magnitudes are often different, probably because of differences in degree of relief from iron stress and light conditions between natural waters and incubations.

Shifts toward larger phytoplankton and more diatoms in ACC water experiments resulted in a final incubation community that was more similar to that found in 'Mixed' waters. In three out of four ACC water experiments the initial community was composed of approximately equal proportions of haptophytes and diatoms and had ~50% Chl a in the >20-μm size fraction (Table 3). By the end of the experiments diatoms dominated, and >20-μm Chl a increased to 75–80%, similar to 'Mixed' waters except for the underrepresentation of haptophytes in incubations. Although these observations are consistent with the hypothesis that the phytoplankton blooms found in 'Mixed' waters result from natural inputs of iron, the community shift in our iron-addition incubations cannot be unambiguously attributed to iron because it was observed in both control and iron treatments. In summary, however, the characteristic biological features that distinguish 'Mixed' from ACC waters are generally elicited by experimental addition of iron to ACC waters, lending support to the hypothesis that natural iron additions from iron-rich shelf water are responsible for the increased phytoplankton biomass observed in 'Mixed' waters.

*Indicators of iron limitation—*Development of physiological or chemical diagnostics of nutrient stress has been a continuing goal of the oceanographic community, particularly for iron limitation. Indicators of iron stress have focused on the photosynthetic systems of phytoplankton, which are sensitive to iron stress because of their high iron requirements. A major direction of this research has been the use of active fluorescence methods to probe PSII function. These techniques have proved valuable in field settings for large-scale surveys where rapid, repetitive measurements are required (e.g., Behrenfeld and Kolber 1999; Suzuki et al. 2002). However, field studies of phytoplankton photosynthetic physiology have primarily examined the extremes of iron limitation and nutrient-replete conditions. In this study, data from iron-addition incubations conducted across a gradient in iron stress are examined for relationships between initial photosynthetic physiological parameters and subsequent responses of phytoplankton to iron addition. This analysis helps identify

Table 5. Regression relations with ILIs, percent of variance explained (r^2), and significance level (p). Relationships significant at the 0.05 level are in bold.

	ILI_{Chl}		ILI_{POC}		ILI_μ	
	r^2	p	r^2	p	r^2	p
$F_v:F_m$	**0.44**	**0.05**	**0.69**	**0.01**	**0.58**	**0.02**
τ^{-1}	0.36	0.08	0.15	0.33	0.02	0.74
p	**0.52**	**0.03**	0.24	0.22	0.29	0.13
σ_{PSII}	**0.66**	**0.01**	**0.56**	**0.03**	0.40	0.06
α^{Chl}	0.01	0.96	0.08	0.62	0.01	0.81
P_{max}^{Chl}	0.02	0.90	0.16	0.39	0.24	0.18
Fe	0.32	0.12	0.42	0.08	**0.65**	**0.01**

and validate the utility of fluorescence- and P vs. E–derived photosynthetic physiological parameters as indicators of degrees of iron stress.

Employing ILIs as metrics for iron stress, significant relationships ($p < 0.05$) were found between initial photosynthetic characteristics and biomass (ILI_{Chl}, ILI_{POC}) and growth rate (ILI_μ) responses to iron addition (Table 5; Fig. 6). FRRF-derived PSII characteristics were found to be the best indicators of iron limitation, especially $F_v:F_m$ and σ_{PSII}, which were sensitive to degrees of iron stress (Fig. 6). Data from all incubations were included for regressions with ILI_{Chl} and ILI_μ, but the data point from incubation A4 was excluded as an outlier for ILI_{POC} correlations. While the value of ILIs change as incubations develop, and even though incubations were of different duration, similar relationships with PSII parameters were found using ILI_{Chl} computed at days 8 and 10 and the final time points, indicating that the relationships determined are robust with respect to temporal changes in ILIs (data not shown). $F_v:F_m$ had significant relationships with all ILIs. While σ_{PSII} was also well correlated with ILI_{Chl} and ILI_{POC}, the relationship with ILI_μ was weaker and was not quite significant at the 0.05 level. The p parameter had a significant relationship with ILI_{Chl} (Fig. 6F), but this relationship may be spurious, as there were no clear trends between p and other ILIs (Table 5).

The trends observed are consistent with the known effects of iron on PSII parameters. Strong responses to iron were found when $F_v:F_m$ was low, and numerous culture and field studies have shown reductions in $F_v:F_m$ under iron stress (e.g., Greene et al. 1992; Suzuki et al. 2002). The association of larger σ_{PSII} with iron-stressed phytoplankton in our study region is consistent with many field and culture studies (Greene et al. 1992; Suzuki et al. 2002), though in some cases a decrease in σ_{PSII} with iron stress has been observed (Vassiliev et al. 1995). Increasing σ_{PSII} may be beneficial under iron stress as an acclimation to maximize
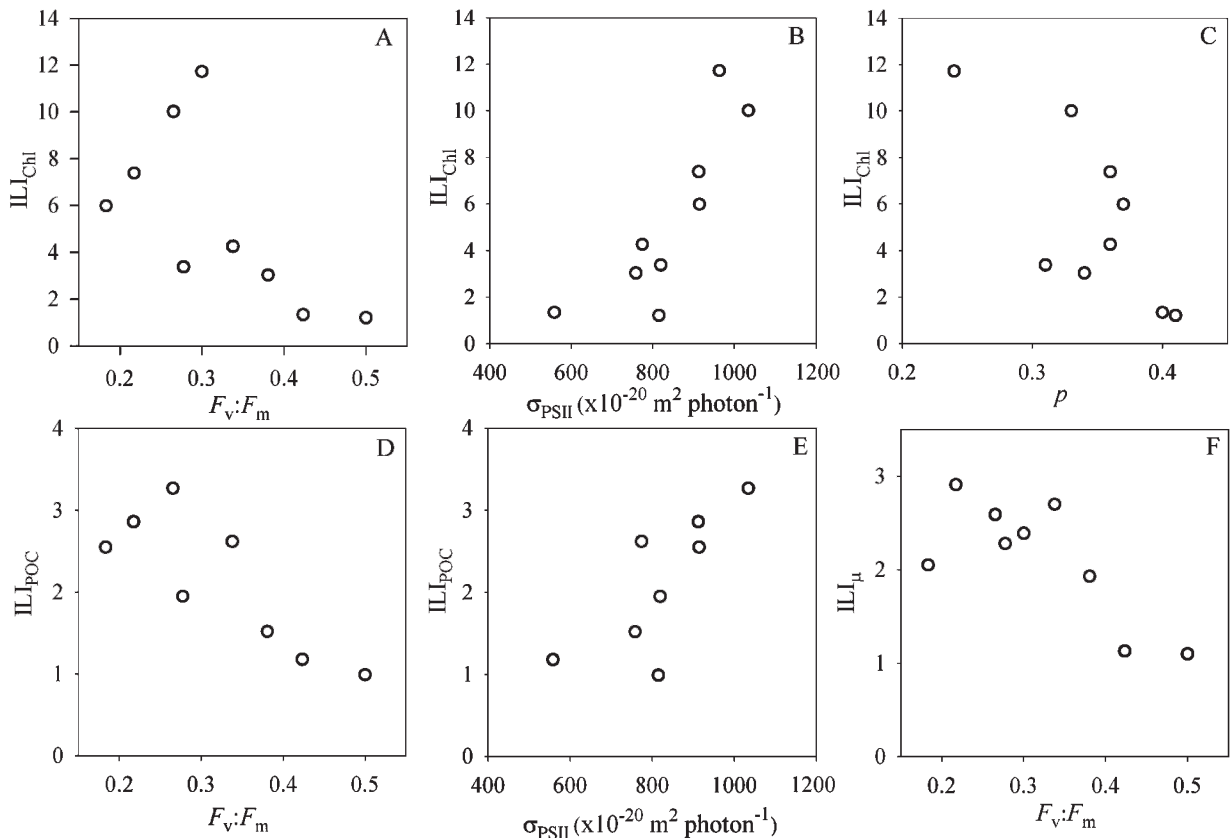

Fig. 6. Indicators of iron limitation. (A, B, C) Plots of iron-limitation indices (ILIs) determined from chlorophyll (ILI_{Chl}); (D, E) POC (ILI_{POC}); and (F) growth rate (ILI_μ) responses to iron in incubation experiments, versus PSII characteristics for which significant linear regression relationships were found. ILI and PSII data used to construct plots are presented in Tables 1 and 2, and regression statistics are summarized in Table 5.

light capture with a minimum number of iron-containing reaction centers (Greene et al. 1992). Because σ_{PSII}, the functional absorption cross section of PSII, is a product of the optical absorption cross section of the PSII antennae complex and $F_v:F_m$, σ_{PSII} and $F_v:F_m$ are not independent parameters (Kolber et al. 1998). However, iron-stress reduced $F_v:F_m$, whereas σ_{PSII} increased, indicating that variability in the optical absorption cross section under changing iron availability controlled the behavior of σ_{PSII}. Measurement of σ_{PSII} adds additional information to assess iron limitation, since σ_{PSII} seems to primarily reflect the optical absorption cross section in the field data and correlates with experimental responses to iron addition. While the correlation between p and ILI_{Chl} may have arisen by chance, the negative relationship observed is consistent with limited culture data showing that p is lowered under iron stress (Greene et al. 1991, 1992; Vassiliev et al. 1995). p is interpreted as a measure of the interconnection between PSII units, although the physiological mechanisms responsible for energy transfer between reaction centers are not well understood (Ley and Mauzerall 1986). Candidate mechanisms, including close physical proximity of reaction centers or sharing of antennae complexes, would be negatively affected by iron limitation as disconnected pigment–protein complexes accumulate and reaction center density decreases. However, alternative explanations for the p parameter and its variability are possible; these include uneven light absorption in densely pigmented cells (Greene et al. 1992) or changing distributions of σ_{PSII} values from different members of the natural phytoplankton community.

Olson et al. (2000) provided the only previous published report of a relationship between initial photosystem parameters and incubation responses to iron addition. They documented a correlation between initial $F_v:F_m$ and the response of $F_v:F_m$ to iron addition in the western Pacific sector of the Southern Ocean. The relationships we find are similar but significant in that we find $F_v:F_m$ can be used to predict biomass and net growth rate limitation by iron. Additionally, the linear relationships found between ILIs and $F_v:F_m$ and σ_{PSII}, as opposed to threshold responses, indicate that these parameters are capable of resolving degrees of iron stress (Fig. 6). This ability to distinguish degrees of iron limitation is important since many systems, including the region of our study and some eastern boundary current systems such as the California Current, are subject to different levels of iron stress with varying consequences for the ecology and biogeochemistry of the waters (Hutchins et al. 1998; Firme et al. 2003).

Other parameters that are known to be influenced by iron stress did not have significant relationships with ILIs, indicating that other environmental factors had a stronger influence on them in this system. Although culture studies show they can be sensitive to iron limitation, the P vs. E parameters, α^{Chl} and P^{Chl}_{max}, had no relationship with degree of iron limitation (Table 5). τ^{-1} was generally smaller at ACC stations, and responses of τ^{-1} to iron addition were observed, but correlations between ILIs and τ^{-1} were not significant (Table 5). Additionally, no significant correlations were found between iron concentrations and ILI_{Chl} or ILI_{POC}, and although a significant correlation occurred

between ILI_μ and iron concentrations, this regression was leveraged solely by the high iron concentrations on the shelf and cannot be considered a useful relationship without data from locations with intermediate iron concentrations. In our study region a disconnect between iron concentrations and iron stress, except at the most general level, likely occurs because introduced iron is rapidly taken up in 'Mixed' waters. Thus, the rate of nutrient supply, which is often difficult to determine, is frequently more important than nutrient concentrations, again emphasizing the need for alternative indicators of nutrient stress.

The observed relationships between PSII parameters and incubation responses to iron addition indicate that phytoplankton iron stress is an important control on photosynthetic physiology in the southern Drake Passage. These correlations do not imply causation, but instead may reflect a codependence of ILIs and PSII parameters with iron availability in the waters. Biochemical consequences of iron stress can be used to rationalize these trends by analogy with responses to iron stress observed in culture experiments. However, other possible confounding factors should be considered before concluding that our correlations do reflect the influences of iron. Nitrogen stress is known to affect PSII in ways similar to iron stress, but nitrate levels were high throughout the region, greater than 20 μmol L^{-1}. Because iron is involved in nitrate uptake, as a cofactor in nitrate reductase (Maldonado and Price 1996), low iron could indirectly result in nitrogen stress reducing photosynthetic competency, but even if this were the case, nitrogen stress would reflect lack of iron and would not invalidate the interpretation of our correlations between ILIs and PSII parameters. High light levels can also influence PSII parameters, but different trends might be expected if photoinhibition were a strong influence. High light generally decreases $F_v:F_m$ and σ_{PSII} together as a result of damage to PSII reaction centers and the need to reduce antennae size to limit light capture, although it is possible that photoinhibition may increase σ_{PSII} if reaction centers are damaged but light harvesting proteins are not reduced, effectively increasing the ratio of antennae to reaction center proteins (Kolber et al. 1988; Falkowski and Kolber 1995). We find increased σ_{PSII} where $F_v:F_m$ is low, a combination observed under iron stress. Diel cycles in $F_v:F_m$ have been observed in the field as a result of photoinhibition and iron stress, potentially influencing the relationships we determined (Behrenfeld and Kolber 1999). Our incubations were generally set up around mid-day, and there was no consistent bias in setup time for any one water type, ruling out time of day as a confounding factor. Other studies have found that phytoplankton community structure can be an important control on σ_{PSII} and can possibly influence other PSII parameters (Moore et al. 2006). However, in the southern Drake Passage we did not find any relationships between the proportion of diatoms or haptophytes in a community and σ_{PSII} or $F_v:F_m$ (all r^2 values < 0.17, $p > 0.3$, $n = 9$). Iron appears to be the primary control on PSII parameters at the depths examined, leading to the observed relationships between these parameters and ILIs, which may be useful for evaluation of iron stress in our study region.

In conclusion, our incubation results support the hypothesis that mixing between iron-limited ACC waters and iron-replete shelf waters occurring in the southern Drake Passage creates the high phytoplankton biomass observed downstream of the mixing region. Iron-addition experiments showed that ACC waters were strongly iron limited, while shelf waters with 1–2 nmol L^{-1} dissolved iron were iron replete. Shelf iron and the physical processes responsible for its introduction into iron-limited waters, as opposed to atmospheric inputs or upwelling of deep iron, are likely important for development of the large blooms observed downstream of islands and the continental protrusions in the Southern Ocean (Sullivan et al 1993).

Using our results from iron-addition experiments conducted throughout a region of strong mixing between iron-limited and iron-replete waters, relationships between degree of iron stress and photosynthetic physiology were found. These results indicate that iron affects certain PSII parameters in this region of the Southern Ocean and that measurement of these parameters can be used to accurately infer iron stress. Other factors known to influence PSII characteristics, including light and nitrogen stress, did not exert strong effects on PSII parameters of natural populations at the depth horizons sampled during our study. Because nitrate levels are high throughout the Southern Ocean and mixed layers are generally relatively deep, thus minimizing photoinhibition, the essential conclusion that PSII parameters reflect degree of iron stress may apply to much of the Southern Ocean.

References

BEHRENFELD, M. J., AND Z. S. KOLBER. 1999. Widespread iron limitation of phytoplankton in the south Pacific Ocean. Science **283:** 840–843.

BLAIN, S., AND OTHERS. 2001. A biogeochemical study of the island mass effect in the context of the iron hypothesis: Kerguelen Islands, Southern Ocean. Deep-Sea Res. I **48:** 163–187.

———, AND OTHERS. 2007. Effect of natural iron fertilization on carbon sequestration in the Southern Ocean. Nature **446:** 1070–1074.

COALE, K. H., AND OTHERS. 2004. Southern Ocean Iron Enrichment Experiment: Carbon cycling in high- and low-Si waters. Science **304:** 408–414.

CULLEN, J. J., AND R. F. DAVIS. 2003. The blank can make a big difference in oceanographic measurements. Limnol. Oceanogr. Bull. **36:** 1578–1599.

DE BAAR, H. J. W., M. A. VAN LEEUWE, R. SCHAREK, L. GOEYENS, K. M. J. BAKKER, AND P. FRITSCHE. 1997. Nutrient anomalies in *Fragilariopsis kerguelensis* blooms, iron deficiency and the nitrate/phosphate ratio (A.C. Redfield) of the Antarctic Ocean. Deep-Sea Res. II **44:** 229–260.

FALKOWSKI, P. G., AND Z. KOLBER. 1995. Variations in chlorophyll fluorescence yields in phytoplankton in the world oceans. Aust. J. Plant. Physiol. **22:** 341–355.

FIRME, G. F., E. L. RUE, D. A. WEEKS, K. W. BRULAND, AND D. A. HUTCHINS. 2003. Spatial and temporal variability in phytoplankton iron limitation along the California coast and consequences for Si, N, and C biogeochemistry. Glob. Biogeochem. Cycles **17:** 1016, doi:10.1029/2001GB001824.

GREENE, R. M., R. J. GEIDER, AND P. G. FALKOWSKI. 1991. Effect of iron limitation on photosynthesis in a marine diatom. Limnol. Oceanogr. **36:** 1772–1782.

———, ———, Z. KOLBER, AND P. G. FALKOWSKI. 1992. Iron-induced changes in light harvesting and photochemical energy conversion processes in eukaryotic marine algae. Plant Physiol. **100:** 565–575.

HABERMAN, K. L., R. M. ROSS, AND L. B. QUETIN. 2003. Diet of the Antarctic krill (*Euphausia superba Dana*): II. Selective grazing in mixed phytoplankton assemblages. J. Exp. Mar. Biol. Ecol. **283:** 97–113.

HELBLING, E. W., V. VILLAFANE, AND O. HOLM-HANSEN. 1991. Effect of iron on productivity and size distribution of Antarctic phytoplankton. Limnol. Oceanogr. **36:** 1879–1885.

HOLM-HANSEN, O., M. KAHRU, AND C. D. HEWES. 2005. Deep chlorophyll a maxima (DCMs) in pelagic Antarctic waters. II. Relation to bathymetric features and dissolved iron concentrations. Mar. Ecol. Prog. Ser. **297:** 71–81.

———, AND B. RIEMANN. 1978. Chlorophyll a determination: Improvements in methodology. Oikos **30:** 438–447.

HUTCHINS, D. A., G. R. DITULLIO, Y. ZHANG, AND K. W. BRULAND. 1998. An iron limitation mosaic in the California upwelling regime. Limnol. Oceanogr. **43:** 1037–1054.

KOLBER, Z., J. ZEHR, AND P. FALKOWSKI. 1988. Effects of growth irradiance and nitrogen limitation on photosynthetic energy conversion in Photosystem II. Plant Physiol. **88:** 923–929.

KOLBER, Z. S., O. PRASIL, AND P. G. FALKOWSKI. 1998. Measurements of variable chlorophyll fluorescence using fast repetition rate techniques: Defining methodology and experimental protocols. Biochim. Biophys. Acta **1367:** 88–106.

LANEY, S. R. 2003. Assessing the error in photosynthetic properties determined by fast repetition rate fluorometry. Limnol. Oceanogr. **48:** 2234–2242.

LEWIS, M. R., AND J. C. SMITH. 1983. A small volume, short-incubation-time method for measurement of photosynthesis as a function of incident irradiance. Mar. Ecol. Prog. Ser. **13:** 99–102.

LEY, A. C., AND D. C. MAUZERALL. 1986. The extent of energy transfer among Photosystem II reaction centers in *Chlorella*. Biochim. Biophys. Acta **850:** 234–248.

MACKEY, M. D., D. J. MACKEY, H. W. HIGGINS, AND S. W. WRIGHT. 1996. CHEMTAX—a program for estimating class abundances from chemical markers: Application to HPLC measurements of phytoplankton. Mar. Ecol. Prog. Ser. **144:** 265–283.

MALDONADO, M. T., AND N. M. PRICE. 1996. Influence of N substrate on Fe requirements of marine centric diatoms. Mar. Ecol. Prog. Ser. **141:** 161–172.

MEASURES, C. I., J. YUAN, AND J. A. RESING. 1995. Determination of iron in seawater by flow injection analysis using in-line preconcentration and spectrophotometric detection. Mar. Chem. **50:** 3–12.

MENDEN-DEUER, S., AND E. J. LESSARD. 2000. Carbon to volume relationships for dinoflagellates, diatoms and other protist plankton. Limnol. Oceanogr. **45:** 569–579.

MITCHELL, B. G., E. A. BRODY, O. HOLM-HANSEN, C. MCCLAIN, AND J. BISHOP. 1991. Light limitation of phytoplankton biomass and macronutrient utilization in the Southern Ocean. Limnol. Oceanogr. **36:** 1662–1677.

MOORE, C. M., AND OTHERS. 2006. Phytoplankton photoacclimation and photoadaptation in response to environmental gradients in a shelf sea. Limnol. Oceanogr. **51:** 936–949.

OLSON, R. J., H. M. SOSIK, A. M. CHEKALYUK, AND A. SHALAPYONOK. 2000. Effects of iron enrichment on phytoplankton in the Southern Ocean during late summer: Active fluorescence and flow cytometric analyses. Deep-Sea Res. II **47:** 3181–3200.

PLATT, T. C., C. L. GALLEGOS, AND W. G. HARRISON. 1980. Photoinhibition of photosynthesis in natural assemblages of coastal marine phytoplankton. J. Mar. Res. **38:** 687–701.

PRICE, N. M. 2005. The elemental stoichiometry and composition of an iron-limited diatom. Limnol. Oceanogr. **50:** 1159–1171.

SARMIENTO, J. L., N. GRUBER, M. A. BRZEZINSKI, AND J. P. DUNNE. 2004. High-latitude controls of thermocline nutrients and low latitude biological productivity. Nature **427:** 56–60.

SEDWICK, P. N., G. R. DITULLIO, AND D. J. MACKEY. 2000. Iron and manganese in the Ross Sea, Antarctica: Seasonal iron limitation in Antarctic shelf waters. J. Geophys. Res. **105:** 11321–11336.

SMITH, W. O., J. MARRA, M. R. HISCOCK, AND R. T. BARBER. 2000. The seasonal cycle of phytoplankton biomass and primary productivity in the Ross Sea, Antarctica. Deep-Sea Res. II **47:** 3119–3140.

SULLIVAN, C. W., K. R. ARRIGO, C. R. MCCLAIN, J. C. COMISO, AND J. FIRESTONE. 1993. Distribution of phytoplankton blooms in the Southern Ocean. Science **262:** 1832–1837.

SUZUKI, K., AND OTHERS. 2002. East-west gradients in the photosynthetic potential of phytoplankton and iron concentration in the subarctic Pacific Ocean during early summer. Limnol. Oceanogr. **47:** 1581–1594.

TIMMERMANS, K. R., AND OTHERS. 2001. Co-limitation by iron and light of *Chaetosceros brevis*, *C. dichaeta* and *C. calcitrans* (Bacillariophyceae). Mar. Ecol. Prog. Ser. **217:** 287–297.

VAN HEUKELEM, L., AND C. S. THOMAS. 2001. Computer-assisted high-performance liquid chromatography method development with applications to the isolation and analysis of phytoplankton pigments. J. Chromatogr. A **910:** 31–49.

VASSILIEV, I. R., Z. S. KOLBER, D. MAUZERALL, V. K. SHUKLA, K. WYMAN, AND P. G. FALKOWSKI. 1995. Effects of iron limitation on Photosystem II composition and energy trapping in *Dunaliella tertiolecta*. Plant Physiol. **109:** 963–972.

VILLAFANE, V. E., E. W. HELBLING, AND O. HOLM-HANSEN. 1995. Spatial and temporal variability of phytoplankton biomass and taxonomic composition around Elephant Island, Antarctica, during the summers of 1990–1993. Mar. Biol. **123:** 677–686.

WRIGHT, S. W., D. P. THOMAS, H. J. MARCHANT, H. W. HIGGINS, M. D. MACKEY, AND D. J. MACKEY. 1996. Analysis of phytoplankton from the Australian sector of the Southern Ocean: Comparisons of microscopy and size frequency data with interpretations of pigment HPLC data using the 'CHEMTAX' matrix factorisation program. Mar. Ecol. Prog. Ser. **144:** 285–298.